MOLECULAR AND CELLULAR BIOLOGY, Nov. 2007, p. 7669–7682 Vol. 27, No. 21
0270-7306/07/$08.00+0 doi:10.1128/MCB.00002-07

Mutation at the Polymerase Active Site of Mouse DNA Polymerase δ Increases Genomic Instability and Accelerates Tumorigenesis[▽]

Ranga N. Venkatesan,[1] Piper M. Treuting,[2] Evan D. Fuller,[1] Robert E. Goldsby,[3] Thomas H. Norwood,[1] Ted A. Gooley,[4] Warren C. Ladiges,[2] Bradley D. Preston,[1] and Lawrence A. Loeb[1]*

Departments of Pathology[1] and Comparative Medicine,[2] University of Washington, Seattle, Washington 98195; Fred Hutchinson Cancer Research Center, Clinical Research Division, D5-360, Seattle, Washington 98109,[4] and Department of Pediatrics, Division of Pediatric Hematology/Oncology, University of California, San Francisco, California 94143-0106[3]

Received 1 January 2007/Returned for modification 5 February 2007/Accepted 16 August 2007

Mammalian DNA polymerase δ (Pol δ) is believed to replicate a large portion of the genome and to synthesize DNA in DNA repair and genetic recombination pathways. The effects of mutation in the polymerase domain of this essential enzyme are unknown. Here, we generated mice harboring an L604G or L604K substitution in highly conserved motif A in the polymerase active site of Pol δ. Homozygous *Pold1*$^{\mathbf{L604G/L604G}}$ and *Pold1*$^{\mathbf{L604K/L604K}}$ mice died in utero. However, heterozygous animals were viable and displayed no overall increase in disease incidence, indicative of efficient compensation for the defective mutant polymerase. The life spans of wild-type and heterozygous *Pold1*$^{\mathbf{+/L604G}}$ mice did not differ, while that of *Pold1*$^{\mathbf{+/L604K}}$ mice was reduced by 18%. Cultured embryonic fibroblasts from the heterozygous strains exhibited comparable increases in both spontaneous mutation rate and chromosome aberrations. We observed no significant increase in cancer incidence; however, *Pold1*$^{\mathbf{+/L604K}}$ mice bearing histologically diagnosed tumors died at a younger median age than wild-type mice. Our results indicate that heterozygous mutation at L604 in the polymerase active site of DNA polymerase δ reduces life span, increases genomic instability, and accelerates tumorigenesis in an allele-specific manner, novel findings that have implications for human cancer.

Eukaryotic DNA polymerase δ (Pol δ) is an essential, highly conserved enzyme that participates in DNA replication, DNA repair, and genetic recombination. Pol δ is believed to replicate a large portion of the genome, synthesizing most of the lagging strand and perhaps contributing to leading-strand synthesis as well (14, 22, 43) The 125-kDa catalytic subunit, encoded at the mouse *Pold1* locus, contains a polymerase domain near the carboxyl terminus that catalyzes DNA synthesis and an exonuclease domain near the amino terminus that catalyzes 3′→5′ exonucleolytic proofreading (5, 18). Pol δ is highly processive in association with PCNA and synthesizes DNA with great accuracy, catalyzing about one error in 10^{-5} to 10^{-6} nucleotides polymerized (11, 46, 61). Discrimination between correct and incorrect base pairs at the polymerase active site confers most of the fidelity (error rate, ca. 1×10^{-5}), while proofreading increases accuracy approximately 10- to 60-fold (11). Partitioning of the newly formed primer terminus between the polymerase and exonuclease active sites is an important determinant of accuracy as well (11, 47). In cells, mismatch repair adds an additional correction mechanism for errors that escape proofreading, reducing the overall error rate to about 1×10^{-9} bp (19, 35, 36, 55).

Accurate DNA replication is essential for the maintenance of genomic stability and suppression of carcinogenesis. Mutants of prokaryotic and eukaryotic DNA polymerases that harbor amino acid substitutions in the polymerase domain or that lack proofreading exhibit increased mutation frequencies in vitro and in vivo (2, 8, 34, 42, 44, 47, 60). In the case of Pol δ, inactivation of the 3′→5′ exonuclease confers a mutator phenotype, increasing mutation rates in haploid yeast and in homozygous mouse embryo fibroblasts (MEFs) (7, 16, 17, 58). The homozygous mutant mice display elevated cancer incidence, suggesting that unrepaired Pol δ errors may contribute to tumorigenesis (16, 17).

Given the essentiality of Pol δ and its central role in eukaryotic DNA replication, it is important to assess the nature and severity of the consequences of polymerase active site mutations in mammals. For this study, we created mice harboring mutations at a conserved Leu residue, L604, in motif A of the Pol δ polymerase domain. We elected to study L604 mutants because the effects on accuracy of mutation at homologous residues in other DNA polymerases have been studied extensively. For example, our laboratory has shown that substitution at the homologous Ile in both *Escherichia coli* Pol I and *Taq* Pol I creates mutator mutants (40, 41, 57). In phage T4 DNA polymerase, substitution for the homologous Leu can generate either mutator or antimutator mutants (47). In yeast and human DNA polymerase α (Pol α), substitution for the orthologous Leu generates mutators of various strengths (38). Most recently, we and others have shown that replacement of L612 in *Saccharomyces cerevisiae* Pol δ with each of eight different amino acids increases spontaneous mutation rates up to 37-fold (28, 62). The L612G and L612K yeast Pol δ alleles, which

* Corresponding author. Mailing address: Department of Pathology, Box 357705, University of Washington, Seattle, WA 98195-7705. Phone: (206) 543-6015. Fax: (206) 543-3967. E-mail: laloeb@u.washington.edu.
▽ Published ahead of print on 4 September 2007.

are homologous to the L604G and L604K mutations we studied here, elevated the mutation rate 17- and 13-fold, respectively (62).

The present work represents the first description of mammals harboring a mutation in the polymerase domain of a major replicative DNA polymerase. Given the significant phenotypic defects we observed in haploid yeast (62) and the central role of Pol δ in replication, it was not certain that the murine L604G and L604K alleles would yield viable animals. However, when heterozygous, these mutator mutations are compatible with mammalian development and reproduction and do not produce a significant overall increase in end-of-life pathology, indicative of extensive compensation for the defective mutant polymerases. Interestingly, both alleles result in a mutator phenotype, and a single *Pold1*^{L604K} allele, but not a *Pold1*^{L604G} allele, accelerates tumorigenesis and reduces life span. We discuss the implications of our results for the ongoing search for Pol δ mutations in human cancers.

MATERIALS AND METHODS

Generation of *Pold1*$^{+/L604G}$ and *Pold1*$^{+/L604K}$ mice. To generate the targeting vectors, sequence-verified wild-type murine *Pold1* genomic DNA (16) was amplified with primers 5′-GTC GCG GAT CCT TCT CTC TGT CTG GGC ATT GGT GA-3′ and 5′-TGT CCC CGC GGC CCA GTA GCC TGC CTT TCC CCAG-3′ spanning exons 9 to 15 (16). The PCR product was digested with SacII and BamHI and cloned into pBluescript II KS digested with the same enzymes. The pBlueEx9-15 vector was used as a template to generate point mutations by site-directed mutagenesis (QuikChange Kit; Stratagene, La Jolla, CA) at Leu604 in exon 15. Leu604 was changed to glycine (L604G) or lysine (L604K), and the entire coding region in the modified vectors was sequenced to verify the presence of mutations at Leu604 and the absence of PCR-generated mutations. A neomycin selection cassette was inserted into each modified vector at the intronic XbaI site between exons 11 and 12, and the vectors were digested with BsaBI and BspEI (naturally occurring sites) to excise most of the coding region spanning exons 9 to 15 (16). The excised fragments were subcloned by replacing the fragment in the vector pBSFN41 containing the genomic coding sequence from exons 2 to 26 to obtain pBSFN43-L604G and pBSFN43-L604K (16). The pBSFN43 vectors were digested with Sal1 to remove the entire pBluescript II KS vector backbone, and the *Pold1* Sal1 fragment was cloned into Xho1-digested TK1-TK2C harboring thymidine kinase coding regions (16) to obtain the *Pold1* targeting vectors TKFN3-L604G and TKFN3-L604K. The TKFN3 vectors were linearized by digestion at a unique NotI site between the thymidine kinase coding regions, purified, and electroporated into R1 embryonic stem (ES) cells (16). The R1 ES cells were derived from 129X1/SvJ × 129S1 F_1 blastocysts (37). Recombinant clones were selected on medium containing G418 and ganciclovir and analyzed by Southern blotting, PCR, and DNA sequencing to confirm *Pold1* locus-specific integration. Two different *Pold1*-targeted ES clones of each genotype were injected into eight-cell-stage C57BL/6J embryos to generate male chimeras, which were crossed with C57BL/6J mice, and offspring were genotyped by PCR to verify germ line transmission. The recombinant mice analyzed in this study were a 50:50 mixture of the B6 and 129 strains. Mice were housed and cared for under the guidelines of the University of Washington Animal Care and Use Committee.

Genotyping and DNA sequencing. Genomic DNA from tail samples was isolated by standard procedures and additionally purified with a QIAquick PCR Purification Kit (QIAGEN, Germantown, MD). PCRs were performed with the Expand Long Template PCR System (Roche, Indianapolis, IN), buffer 1, 1.5 μl (~100 ng) of purified genomic DNA, and primers L1 (5′-CCTGGCACTGCTG GAGGAAATAGAGG-3′) and L2 (5′-CAGGTCGGTGATGATGCTGTGCT GAA-3′) in an MJ Research PTC-200 thermocycler under the following cycling conditions: 95°C for 2 min, followed by 11 cycles of 95°C for 30 s, 63°C for 30 s, and 68°C for 3 min. The next 20 cycles were the same, but the 68°C extension time was increased by 20 s with each cycle, with a final incubation at 68°C for 7 min. For routine genotyping, primers Ex11F (5′-GACTGGTCTCCGCTCCAA CATCCGTGA-3′) and Ex16R (5′-GAGGCCCTTCCGTACAGATGACTTCA CAAA-3′) were amplified essentially as described above under the following cycling conditions: 95°C for 2 min, followed by 10 cycles of 95°C for 30 s, 63°C for 30 s, and 68°C for 2 min. The next 20 cycles were the same, but the 68°C extension time was increased by 20 s with each cycle, with a final incubation at 68°C for 7 min.

For Southern blot analyses, ~30 μg of genomic DNA from *Pold1*-targeted ES clones was digested with HindIII or HindIII and SphI, resolved on a 1% agarose gel, transferred to a neutral nylon membrane, probed with a 5′ probe (see Fig. 1) labeled with [α-^{32}P]dCTP (3,000 Ci/mmol; Amersham) with the random primed DNA labeling kit (Roche, Indianapolis, IN), and visualized by phosphorimaging.

PCR products were purified with a MultiScreen PCR96 filter plate (Millipore, Billerica, MA), and automated DNA sequencing was performed in the Department of Biochemistry, University of Washington, sequencing facility. Sequences were analyzed with DNA Sequencher software.

Analysis of Pol δ expression. Expression of Pol δ was analyzed by Western blotting of liver whole-cell extracts. Liver collected at necropsy was frozen in dry ice and determined to be histologically normal prior to use. Tissue (100 to 110 mg) was homogenized in 2 ml of phosphate-buffered saline (PBS), pH 7.5, supplemented with 1% NP-40, 0.5% deoxycholate, 0.1% sodium dodecyl sulfate (PBS-radioimmunoprecipitation assay buffer) supplemented with 1× protease inhibitor cocktail set III (Calbiochem, San Diego, CA) and extracted on ice for 20 min. The extract was spun at 14,000 rpm at 4°C for 20 min, and the clear whole extracts were carefully removed and flash frozen in liquid nitrogen in small aliquots. Protein content was quantitated by using a BCA protein assay kit (Pierce, Rockford, IL). Aliquots were subjected to 8% sodium dodecyl sulfate-polyacrylamide gel electrophoresis and transferred to a nitrocellulose membrane, and the membrane was blocked with 10 mM Tris-HCl (pH 7.5)–150 mM NaCl–0.1% Tween 20–5% nonfat dry milk. The membrane was probed overnight with a 1:700 dilution of Pol δ antibody sc-8797 (Santa Cruz Biotechnology Inc., Santa Cruz, CA) in the same buffer as described above and developed by enhanced chemiluminescence with the Pierce SuperSignal WestPico substrate (Pierce, Rockford, IL). The Pol δ signal was removed by incubating the membrane in Restore Western blot stripping buffer (Pierce, Rockford, IL) for 30 min at room temperature, blocked as described above, probed overnight with a 1:1,000 dilution of tubulin antibody YOL1/34 (Novus Biologicals, Littleton, CO), and developed by enhanced chemiluminescence as described above.

Determination of spontaneous mutation rates. MEFs were harvested from day 11.5 to 13 embryos and cultured in αMEM (Mediatech, Inc., Herndon, VA) supplemented with 10% fetal bovine serum (HyClone, Logan, UT), penicillin-streptomycin-glutamine, and amphotericin B (Fungizone; Invitrogen, Carlsbad, CA). After the first passage, primary MEFs were immortalized by infection with retrovirus expressing the EIA oncogene, and two different immortalized lines of each genotype were used for mutation analysis. Spontaneous mutation rates were measured in duplicate or triplicate by Luria-Delbruck fluctuation analysis by the method of the mean. Cells (50 to 200) were seeded in six-well plates and cultured for 13 to 15 days or until the average cell density was ~0.9 to 1.2 million cells/well. Cells from each well were trypsinized, transferred to a 10-cm plate, and propagated for 48 h; the average cell density at this stage was ~4 to 6 million cells/plate. Cells from six 10-cm plates were trypsinized, pooled, and counted thrice with a hemocytometer. A small aliquot of cells was serially diluted to assess plating efficiency, and the remainder was seeded at 450,000 cells/plate in medium containing 5 μg/ml 6-thioguanine (Sigma, St. Louis, MO) to select for 6-thioguanine-resistant clones. The medium was changed every fourth day, and on day 15 all plates were stained with crystal violet and colonies containing more than 40 cells were counted.

Chromosome analysis. Primary MEFs, derived from day 11 to 13 embryos and frozen after passage 1, were reestablished in culture. For each genotype, three or four different early-passage cell lines derived from two or three different crosses were used for chromosome analysis. After a lag period of ca. 28 h, when a large fraction of cells were observed to be mitotically active, Colcemid (0.5 μg/ml of medium; Sigma, St. Louis, MO) was added and incubation was continued for 35 min. The cells were pelleted gently, and the pellet was suspended in 8 ml of prewarmed hypotonic buffer and incubated at 37°C for 22 min. Cells were pelleted and suspended in 0.5 ml of methanol-acetic acid (3:1) and spun down gently. The cell pellet was suspended in 5 ml of methanol-acetic acid (3:1) and stored at 4°C. The fixed cells were processed for C-banding analysis by standard cytogenetic techniques, and a minimum of 1,000 chromosomes from each cell line was analyzed for aberrations in a blinded manner.

Flow cytometric analysis of γ-H2AX stained cells. Early-passage (passage 2) MEFs were established from frozen stocks and expanded by one additional passage, and ~100,000 cells were seeded into 6-cm plates. After 24 h, cultures were treated with aphidicolin (0.4 μg/ml or 4 μg/ml), hydroxyurea (0.4 mM or 4 mM), or the carrier, dimethyl sulfoxide, for 8 h. Cells were dislodged by treatment with trypsin-EDTA, washed twice with ice-cold PBS, fixed in 1 ml ice-cold 70% ethanol, and stored at −20°C. Fixed cells were diluted to 30% ethanol by addition of Tris-buffered saline (TBS; 20 mM Tris-HCl [pH 7.4], 150 mM NaCl), centrifuged at 10,000 rpm for 4 min, washed once with cold TBS-T (TBS plus 4% fetal bovine serum and 0.1% Triton X-100), resuspended in 0.5 ml TSB-T, and placed on ice for 10 min. Cells were then centrifuged, resuspended in 0.2 ml of anti-phosphoserine H2AX antibody (Millipore, Bedford, MA) diluted 1:500 in TBS-T, and agitated for 2 h at room temperature. They were then washed once with TBS-T, resuspended in 0.2 ml of Alexa 488-conjugated goat anti-mouse immunoglobulin G (heavy plus light chains) secondary antibody (Invitrogen, Carlsbad, CA) diluted 1:200 in TBS-T, and agitated for 1 h at room temperature. After being washed once with TBS-T, cells were resuspended in TBS–4′,6′-diamidino-2-phenylindole (DAPI; 3 μg/ml; Sigma, St. Louis, MO), gently vortexed, pushed through a G-25 needle, and sorted on a Cytopeia (Seattle, WA) cell sorter. As a control, cells were also stained with anti-NeuN, an unrelated antibody (Millipore, Billerica, MA), according to the manufacturer's directions. Sorted cells were analyzed with FSC Express software (Thornhill, Ontario, Canada).

Histology. Samples were collected from all soft tissues during necropsy and fixed in neutral buffered formalin. The tissues were embedded in paraffin, sectioned, stained with hematoxylin and eosin, and examined by light microscopy. Each tissue was given a morphological diagnosis, after which the common non-neoplastic lesions and all neoplastic processes were graded as described by Ikeno et al., with modifications (24). Neoplastic processes were morphologically diagnosed, and each primary tumor was assigned a neoplastic score based on the extent of tumor size and distribution (metastasis) within the tissues examined. Grade 1 tumors included small focal tumors contained within the primary site. Grade 2 tumors had intraorgan or one other organ metastasis. Grade 3 tumors had metastatic foci in two or three organs. Grade 4 tumors had metastases to more than four organs or were grade 3 with additional pathology. Primary tumor scores were then summed to assign the total neoplastic burden for the animal when more than one primary tumor was present. Only tumors with a minimum grade of 1 were scored.

RESULTS

Generation of *Pold1*$^{+/L604G}$ and *Pold1*$^{+/L604K}$ mice. Based on homology with mutator mutants of yeast Pol δ and prokaryotic DNA polymerases, we chose Leu604 in the Pol δ catalytic subunit as a target for the creation of mutator mice (40, 57, 62). Leu604 is located in highly conserved motif A in the active site of the polymerase domain (Fig. 1A), and Leu is found at this position in all reported eukaryotic Pol δ sequences (Fig. 1B). As exemplified in Fig. 1C, the structure of the family B DNA polymerase active site has been conserved throughout evolution, although the primary sequence varies. We changed Leu604 to either glycine (L604G) or lysine (L604K) by using site-specific mutagenesis. Targeting vectors containing the mutated alleles were electroporated into R1 (129X1/SvJ × 129S1) ES cells to undergo homologous recombination at the *Pold1* locus (Fig. 2A). Locus-specific targeting was verified by Southern blotting and by PCR amplification and sequencing of DNA from heterozygous *Pold1*$^{+/L604G}$ and *Pold1*$^{+/L604K}$ ES cells (Fig. 2B to D). The amounts of Pol δ in liver extracts from wild-type and heterozygous animals were determined by Western blotting, as exemplified in Fig. 2E; comparable expression was observed in mice at 9 to 20 months of age. These data indicate that the mutant alleles were targeted to the *Pold1* locus and suggest that the mutant and wild-type proteins were expressed at similar levels. Two different ES clones of each heterozygous genotype were injected into C57BL/6 blastocysts that were then implanted into pseudopregnant females to generate male chimeras. The chimeras were mated with wild-type C57BL/6 animals, and heterozygous F_1 offspring (50% mixture of strains B6 and 129) were identified by genotyping. Five F_1 *Pold1*$^{+/L604G}$ × *Pold1*$^{+/L604G}$ and eight *Pold1*$^{+/L604K}$ × *Pold1*$^{+/L604K}$ breeding pairs were used to generate F_2 animals, composed of 71 heterozygous *Pold1*$^{+/L604G}$ and 31 wild-type *Pold1*$^{+/+}$ animals and 132 heterozygous *Pold1*$^{+/L604K}$ and 36 wild-type *Pold1*$^{+/+}$ animals, respectively. The heterozygous *Pold1*$^{+/L604G}$ and *Pold1*$^{+/L604K}$ mice were healthy and fertile. No homozygous mutant animals were obtained, a result we extended by genotyping embryos from test (heterozygous × heterozygous) breeders of *Pold1*$^{+/L604G}$ and *Pold1*$^{+/L604K}$ mice. No homozygous mutant embryos were detected among a minimum of 12 embryos harvested from *Pold1*$^{+/L604K}$ mice on days 12.5, 10.5, and 8.5 postfertilization and a minimum of 6 embryos harvested from *Pold1*$^{+/L604G}$ mice on days 13.5, 11.5, and 10 postfertilization, indicating that, when homozygous, both alleles cause early embryonic lethality.

Mutator phenotypes of *Pold1*$^{+/L604G}$ and *Pold1*$^{+/L604K}$ cultured MEFs. To determine whether heterozygosity for the *Pold1*$^{+/L604G}$ and *Pold1*$^{+/L604K}$ alleles confers a mutator phenotype, we measured spontaneous mutation rates in MEFs. Wild-type and heterozygous fibroblast lines were established from 11- to 13-day-old embryos and immortalized at first passage by infection with a retrovirus harboring the E1A oncogene. Primary and immortalized MEFs from both wild-type and heterozygous mice exhibited the same doubling times. Spontaneous mutation rates were ascertained at the hypoxanthine-guanine phosphoribosyltransferase (*Hprt*) locus, measured as the number of 6-thioguanine-resistant mutants/cell/generation (53). For each genotype, mutation rates were measured in two different cell lines established from each of two different animals. The spontaneous mutation rate was elevated fourfold in *Pold1*$^{+/L604K}$ cells and fivefold in *Pold1*$^{+/L604G}$ cells, relative to the wild-type rate (Table 1), indicating that a single copy of the mutant Pol δ allele in heterozygous mouse cells is sufficient to increase mutagenesis. Because MEFs have a tendency to become tetraploid during the process of immortalization, it is likely that the observed mutation rates are an underestimate due to polyploidy of the X chromosome.

To assess whether the mutant polymerase alleles cause chromosome instability, we analyzed C-banded metaphase spreads from primary (passage 2) MEFs. The number of chromosome aberrations was elevated 17-fold in *Pold1*$^{+/L604G}$ cells ($P < 0.02$) and 38-fold in *Pold1*$^{+/L604K}$ cells ($P < 0.001$), relative to wild-type fibroblasts, as indicated in Fig. 3A. The abnormalities consisted predominantly of chromatid and chromosome gaps and breaks, as illustrated in Fig. 3B, although translocations, radials, acentric fragments, and ring and dicentric chromosomes were also seen. These data indicate that a single copy of the mutant Pol δ alleles results in chromosomal instability. We conclude that, when heterozygous, the *Pold1*^{L604G} and *Pold1*^{L604K} alleles cause a mutator phenotype at the chromosome level.

Phosphorylation of histone H2AX in wild-type and mutant MEFs. To determine whether the increased spontaneous genomic instability in *Pold1*$^{+/L604G}$ and *Pold1*$^{+/L604K}$ MEFs was accompanied by activation of a DNA damage response, we assessed Ser139 phosphorylation of H2AX (γ-H2AX) as a marker for S-phase checkpoint activation (50). γ-H2AX foci are rapidly formed in the chromatin flanking double-strand breaks caused by endogenously generated replication fork collapse, DNA fragmentation associated with apoptosis, ionizing radiation, and other genotoxic agents (48, 49, 63). Examples of focus formation in *Pold1*$^{+/L604G}$ and *Pold1*$^{+/L604K}$ MEFs are

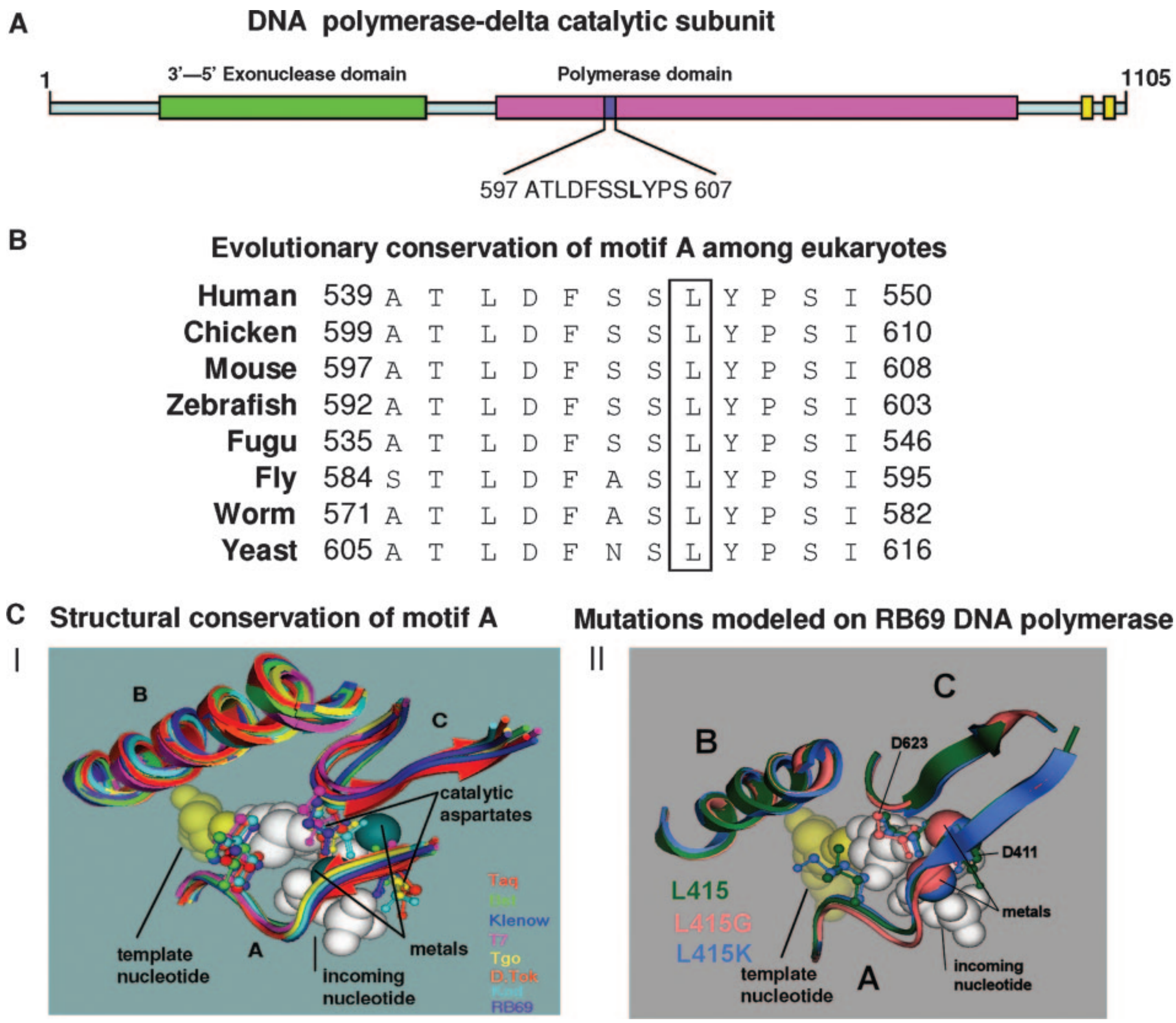

FIG. 1. Primary sequence and structural conservation of the Pol δ active site. (A) Domain structure of murine Pol δ. The exonuclease proofreading domain is located in the amino-terminal region, the polymerase domain occupies the central region, and a putative zinc coordinating domain is located near the carboxy terminus. (B) Sequence alignment of motif A. Primary sequences were aligned by CLUSTALW (http://align.genome.jp/). (C, part I) Conservation of the three-dimensional structure of motif A among DNA polymerases. Coordinates of crystal structures were downloaded from the Protein Data Bank (www.rcsb.org) and manipulated in a suite of programs available in the Molecular Operating Environment package at http://www.chemcomp.com/. The polymerase domains shown are from *Thermus aquaticus* (KlenTaq, 3KTQ) *Bacillus stearothermophilus (Bst*, 1XWL), *E. coli* (Klenow, 1KFD), bacteriophage T7 (T7, 1T7P), *Thermococcus gorgonarius* (Tgo, 1TGO), "*Desulfurococcus tok*" (D.Tok, 1QQC), "*Pyrococcus kodakaraensis*" (Kod, 1GCX), and bacteriophage RB69 (RB69, 1IG9). Motifs A, B, and C were aligned with the ternary structure of the RB69 DNA polymerase. The essential catalytic aspartic acids in motifs A and C that coordinate metal ions are shown. The orthologous motif A residues corresponding to mouse Leu604 (see panel B) are shown making contact with the incoming dNTP. (C, part II) Molecular modeling of motif A mutations L415G and L415K on the ternary structure of the RB69 DNA polymerase. L415G and L415K are orthologous to murine Pol δ L604G and L604K, respectively. Molecular modeling was performed by using Engh and Huber structural parameters and the software described above (9).

shown in Fig. 4C. We used fluorescence-activated cell sorting (FACS) of γ-H2AX-stained cells to examine both untreated MEFs and MEFs treated with aphidicolin or hydroxyurea. Aphidicolin is an inhibitor of DNA polymerases α, δ, and ε (65), while hydroxyurea is an inhibitor of ribonucleotide reductase that results in reduced concentrations of deoxynucleoside triphosphate (dNTP) pools (52). The response to hydroxyurea is of particular interest in view of the hypersensitivity of haploid yeast Pol δ L612G and L612K mutants to this agent (62).

For FACS analysis, we subtracted a background level of fluorescence that excluded essentially all wild-type and mutant cells that stained positive with a nuclear antibody unrelated to γ-H2AX. Such *Pold1*$^{+/L604K}$ cells are shown in Fig. 4A (far left profile), and the threshold fluorescence intensity (gating) is indicated by the lower green line in all four profiles. We observed that, when stained with antibody against γ-H2AX, wild-type, *Pold1*$^{+/L604G}$, and *Pold1*$^{+/L604K}$ MEFs did not differ significantly in the fraction of positive cells, i.e., 0.4%, 0.6%, and 0.4%, respectively. Use of a lower threshold fluorescence in-

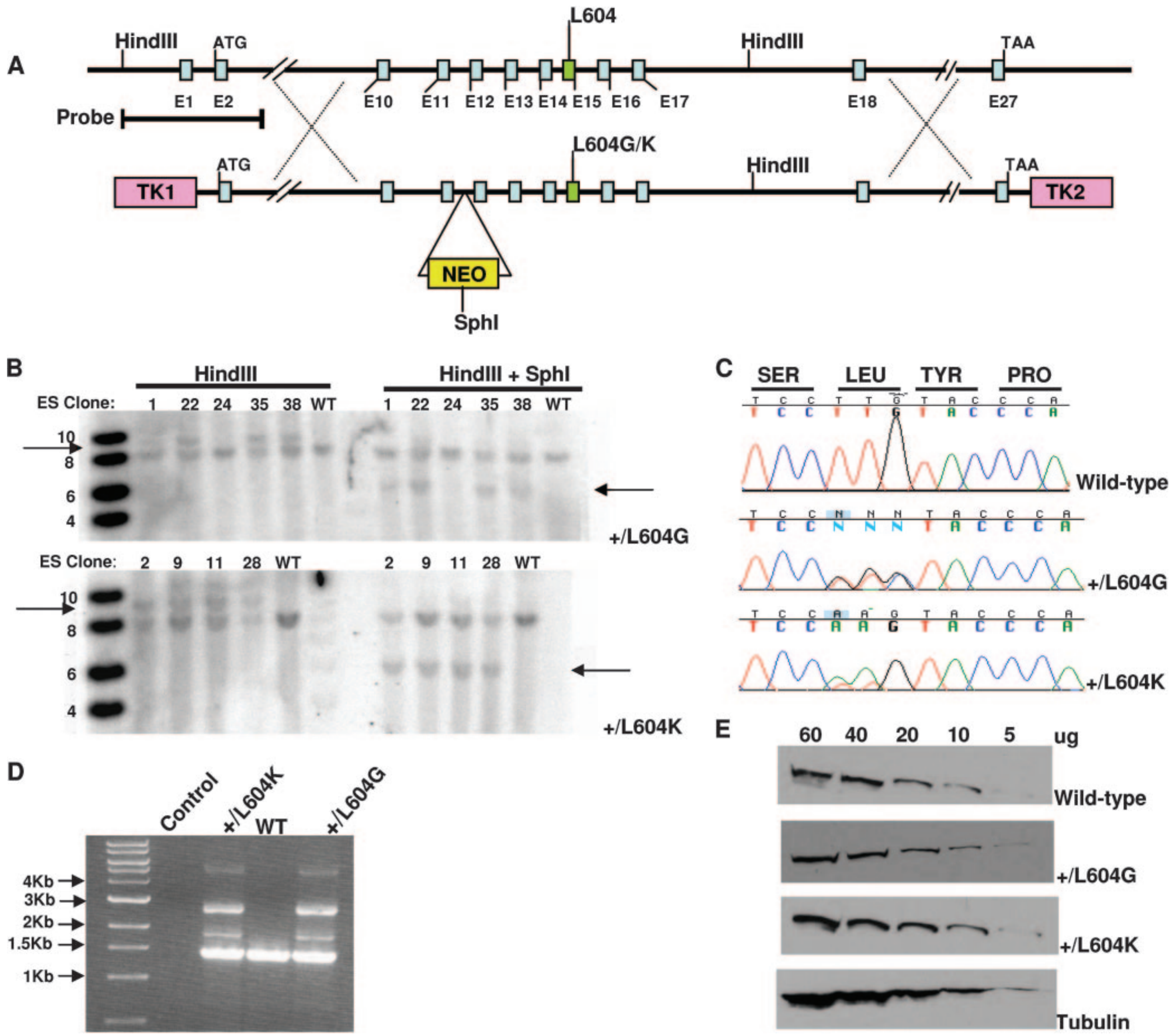

FIG. 2. Generation and verification of *PoldI*$^{+/L604G}$ and *PoldI*$^{+/L604K}$ mice. (A) The structure of the murine *Pold1* locus is shown above the targeting vector. Gray numbered boxes represent exons. A neomycin selection cassette was inserted into intron 11. TK1 and TK2 represent thymidine kinase genes. Targeting vectors carrying the motif A mutation L604G or L604K were generated by site-specific mutagenesis of the corresponding codon in exon 15. (B) Southern blotting of PCR-screened *Pold1*-targeted ES clones. Digestion with HindIII yields 9.3-kb and 8-kb bands, while digestion with HindIII and SphI yields 8-kb and 6.2-kb bands. The numbers at the top of refer to different ES clones. (C) DNA sequence verification of *Pold1*-targeted heterozygous clones. (D) PCR confirmation of heterozygous clones. The top ~3-kb band is the targeted allele, and the bottom 1.5-kb band is the wild type (WT). (E) Expression of Pol δ in whole-cell extracts of liver. Aliquots of extracts containing 5 μg to 60 μg of total protein were applied to gels, and Western blots were probed with anti-Pol δ and antitubulin antibodies.

TABLE 1. Mutation rates in Pol δ mutant embryonic fibroblasts[a]

Genotype	Mutation rate (10^{-8})	Fold elevation
Pold1$^{+/+}$	4 ± 2 (5)	
Pold1$^{+/L604G}$	20 ± 10 (6)	5
Pold1$^{+/L604K}$	17 ± 10 (5)	4

[a] Spontaneous mutation rates (mean ± standard error) at the *Hprt* locus were determined by fluctuation analysis by the method of the mean and are expressed as the number of 6-thioguanine-resistant mutants/cell/generation. Two different cell lines derived from different animals were used for each genotype. Plating efficiencies were similar in all lines and were not adjusted. Unless specified otherwise, the value in parentheses is the total number of times the experiment was performed.

tensity also revealed no significant difference among the three genotypes (data not shown). We then treated cells with replication inhibitors to ascertain whether they might act synergistically with endogenous replication stress created by mutant DNA polymerases to reveal a difference between wild-type and mutant cells. When treated with 0.4 μg/ml and 4 μg/ml aphidicolin, wild-type, *Pold1*$^{+/L604G}$, and *Pold1*$^{+/L604K}$ cultures exhibited similar, progressively elevated fractions of positive cells (1.6%, 1.7%, and 2.7% for 0.4 μg/ml and 12%, 8.5%, and 9.5% for 4 μg/ml, respectively) (Fig. 4B). When treated with 0.4 mM and 4 mM hydroxyurea, a larger percentage of γ-H2AX-

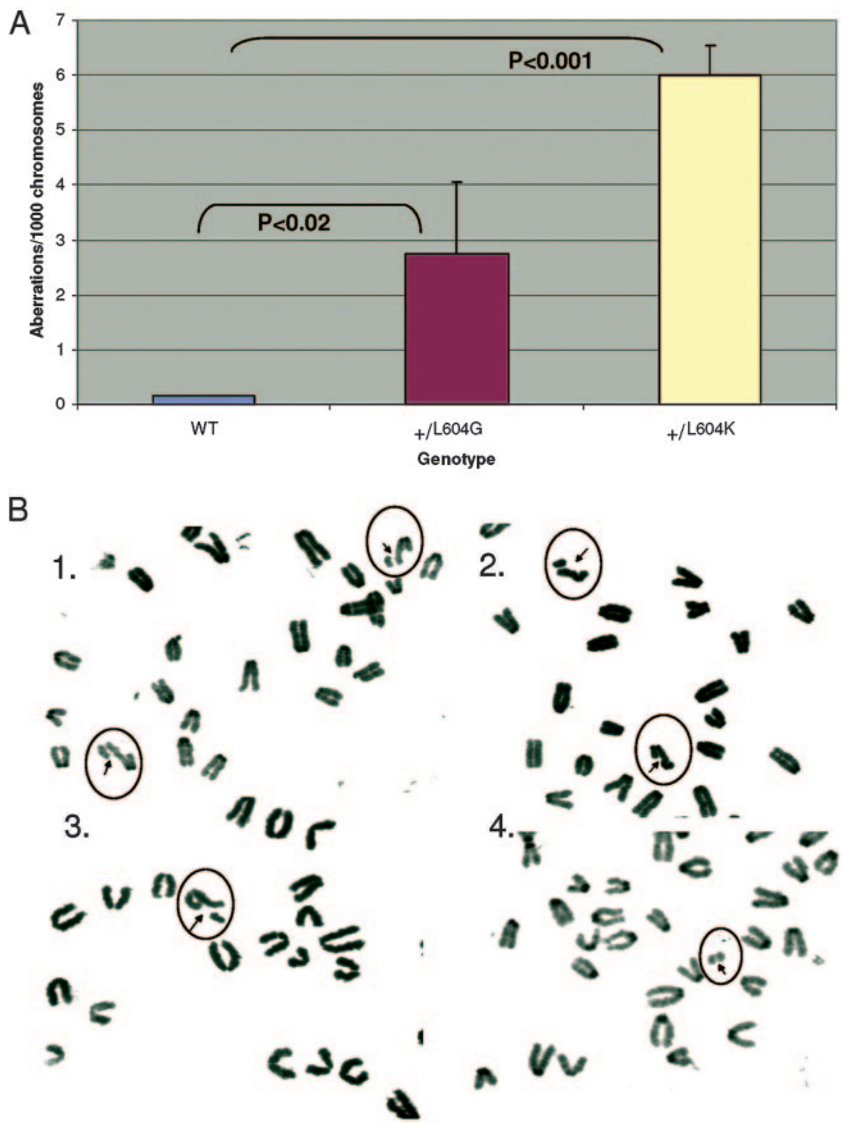

FIG. 3. Chromosome instability in cultured primary embryonic fibroblasts. (A) Total numbers of spontaneous chromosome aberrations observed in wild-type fibroblasts and in *Pold1*$^{+/L604G}$ and *Pold1*$^{+/L604K}$ heterozygous fibroblasts. C-banding metaphase spreads of three different *Pold1*$^{+/+}$ cell lines, four different *Pold1*$^{+/L604G}$ lines, and three different *Pold1*$^{+/L604K}$ lines (passage 2) were used for analysis. A minimum of 1,000 chromosomes was analyzed for each line. *P* values were calculated by unpaired Student *t* test. (B) Commonly observed aberrations in heterozygous lines. Arrows indicate chromatid breaks (parts 1 to 3) and an acentric fragment (part 4).

stained cells was observed in all genotypes (e.g., see the profile of L604K cells in Fig. 4A), and again, the three genotypes did not differ significantly in the fraction of positive cells (26%, 23%, and 28% for 0.4 mM and 29%, 22%, and 33% for 4 mM, respectively) (Fig. 4B). For each treatment condition, we observed no significant differences between the genotypes in the mean intensity per cell or the cell cycle distribution of positive cells (data not shown).

Based on the foregoing results, we conclude the following. (i) Heterozygous L606G and L604K MEFs do not display a spontaneously elevated level of γ-H2AX focus formation. (ii) Wild-type and heterozygous mutant MEFs display comparable levels of focus formation in response to aphidicolin and hydroxyurea and are proficient in DNA damage-induced checkpoint activation. (iii) Drug-induced replication stress and attendant damage in the mutant cells do not interact synergistically with spontaneous replication stress/damage to elevate γ-H2AX focus formation to a level above that in wild-type cells.

Reduced life span of heterozygous *Pold1*$^{+/L604K}$ mice. To assess the effect of the *Pold1*$^{+/L604G}$ and *Pold1*$^{+/L604K}$ alleles on longevity, we measured the life spans of mutant and wild-type mice. Kaplan-Meier survival curves for the three cohorts are shown in Fig. 5. The median survival time of *Pold1*$^{+/L604G}$ mice was 22 months, the same as for wild-type animals. In contrast, the median life span of the *Pold1*$^{+/L604K}$ mice was reduced to 18 months; the decreased survival probability observed for the *Pold1*$^{+/L604K}$ mice is significantly different from that for the wild-type or *Pold1*$^{+/L604G}$ mice ($P < 0.0001$, log rank and Wilcoxon tests). The mean life span of the *Pold1*$^{+/L604K}$ mice (18 months) was also

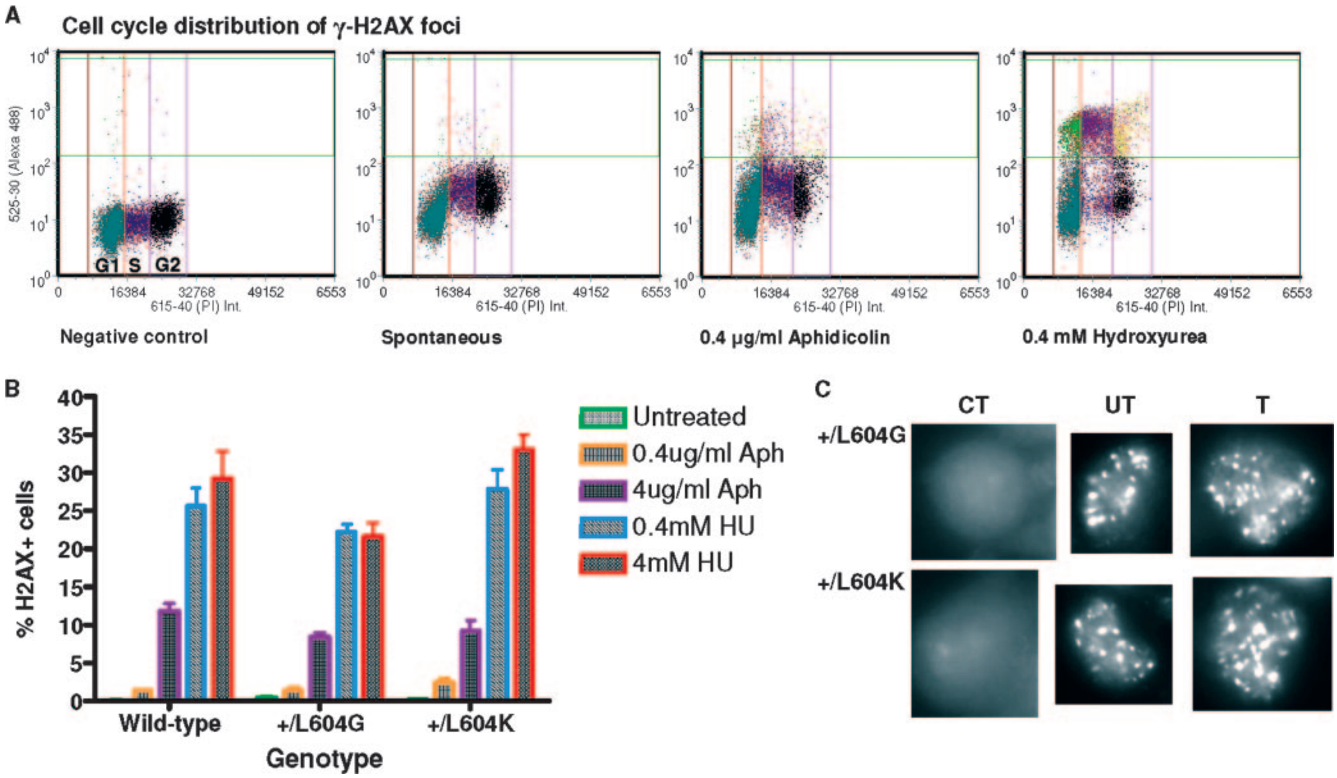

FIG. 4. DNA damage-induced checkpoint response is proficient in *Pold1*$^{+/L604K}$ and *Pold1*$^{+/L604G}$ MEFs. Ser139 phosphorylation of histone variant H2AX was analyzed as a marker for checkpoint response in MEFs derived from wild-type, *Pold1*$^{+/L604G}$, and *Pold1*$^{+/L604K}$ mice. (A) Cell cycle distribution of γ-H2AX foci. The distribution of singlet gated *Pold1*$^{+/L604K}$ cells is shown, with and without treatment with replication inhibitors. Negative control, untreated cells stained with an unrelated nuclear antibody; spontaneous, untreated cells stained for γ-H2AX; 0.4 μg/ml aphidicolin (Aph), cells treated for 8 h with drug and stained for γ-H2AX; 0.4 mM hydroxyurea (HU), cells treated for 8 h with drug and stained for γ-H2AX. Cells above the light green line were used for the analysis in panel B. (B) Fraction of cells positive for γ-H2AX in untreated cells and cells treated with replication inhibitors. For each sample, ~32,000 cells were sorted and ~20,000 cells were used for analysis. (C) Indirect immunofluorescence of γ-H2AX foci in nuclei of *Pold1*$^{+/L604G}$ and *Pold1*$^{+/L604K}$ MEFs. CT, control showing staining with irrelevant antibody; UT, cells not treated with replication inhibitor showing spontaneous focus formation; T, cells treated with 0.4 μg/ml aphidicolin for 8 h. Images were collected at ×63 magnification.

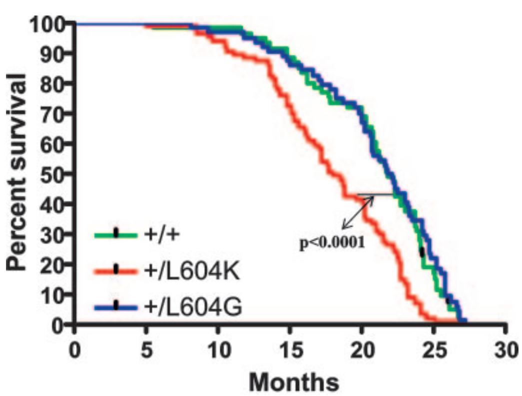

Lifespan	+/+	+/G	+/K
Median	21.9	21.9	17.9
Mean	21.1	21.1	17.9
Max	29.9	27.2	26.9
Min	5.6	8.2	5.6

FIG. 5. Survival of heterozygous Pol δ L604K and L604G mice. Kaplan-Meier survival curves for combined F_1 and F_2 generation *PoldI*$^{+/L604G}$ mice and *PoldI*$^{+/L604K}$ mice are shown. Sixty-one *PoldI*$^{+/+}$ (24 male, 37 female), 64 *PoldI*$^{+/L604G}$ (30 male, 34 female), and 87 *PoldI*$^{+/L604K}$ (44 male, 43 female) animals were used. The life span of *PoldI*$^{+/L604K}$ mice was significantly shorter than that of the combined *PoldI*$^{+/+}$ and *PoldI*$^{+/L604G}$ mice ($P < 0.0001$, log rank and Wilcoxon tests). The median survival time of the +/L604K heterozygotes was 18 months, relative to 22 months for the wild-type and +/L604G animals.

observed to differ from that of the wild-type and *Pold1*$^{+/L604G}$ mice (21 months). The maximum life span of 27 months observed for both the heterozygous *Pold1*$^{+/L604G}$ and *Pold1*$^{+/L604K}$ mice was reduced relative to 30 months for the *Pold1*$^{+/+}$ mice. As indicated in Fig. 5, there was no apparent difference in the survival of *Pold1*$^{+/+}$, *Pold1*$^{+/L604G}$, and *Pold1*$^{+/L604K}$ animals until 11 months of age, after which there was an increase in the mortality rate of the *Pold1*$^{+/L604K}$ mice. These data indicate that a single copy of the Pol δ L604K allele reduces longevity.

Accelerated tumorigenesis in *Pold1*$^{+/L604K}$ mice. We performed a detailed histopathologic analysis of the majority of the mice used in the life span study in order to assess tumor incidence and type. Animals excluded from the tumor study died unexpectedly overnight and were therefore not suitable for tissue analysis due to autolysis, particularly of necrotic tissue. The most commonly diagnosed neoplasms were similar across genotypes and included lymphoreticular tumors (mainly lymphomas), hepatocellular tumors (adenomas and carcinomas of the liver), and bronchiolo-alveolar tumors (adenomas and carcinomas of the lung) (Table 2). The majority of neoplasms in all three genotypes were metastatic (79% to 85%).

We observed a larger proportion of animals with tumors in both heterozygous mutant strains, i.e., 78% in *Pold1*$^{+/L604G}$

TABLE 2. Tumor incidence and type in $Pold1^{+/+}$, $Pold1^{+/L604G}$, and $Pold1^{+/L604K}$ mice[a]

Strain	Total mice	Mice with tumors	Mice with no tumors	Mice with malignant tumors	Mice with multiple tumors	Neoplasms/mouse	Tumor types	No. (%) of: Epithelial tumors	Bronchiolo-alveolar tumors	Hepatocellular tumors	Other tumors	Mesenchymal tumors	Lymphoreticular tumors	Other tumors
Wild type	47 (100)	29 (62)	18 (38)	23 (79)[b]	9 (19)	1.8	10	20 (43)	6 (13)	11 (23)	3 (6)	17 (36)	14 (30)	3 (6)
L604G	59 (100)	46 (78)	13 (22)	39 (85)[b]	15 (25)	2.2	11	33 (56)	11 (19)	19 (32)	3 (5)	31 (53)	26 (44)	5 (8)
L604K	64 (100)	45 (70)	19 (30)	37 (82)[b]	6 (9)	1.9	13	23 (36)	8 (13)	10 (16)	5 (8)	28 (44)	22 (34)	6 (9)

[a] The number and percentage of affected mice are shown.
[b] Percentage of mice with tumors.

mice and 70% in $Pold1^{+/L604K}$ mice versus 62% in wild-type animals (Table 2), although these differences were not statistically significant. We note, however, that the incidence reported for $Pold1^{+/L604K}$ mice may be underestimated. This is so because a disproportionately large fraction of the 11- to 22-month-old $Pold1^{+/L604K}$ animals that were not available for histopathology showed signs of tumors while still alive (not sufficiently serious to warrant sacrifice) and bore suspected tumors upon autopsy that could not be definitively diagnosed because of autolysis (23/87 $Pold1^{+/L604K}$ versus 7/61 $Pold1^{+/+}$; $P = 0.04$, Fisher's exact test). To assess the suggestion from the life span study that tumors may develop at an earlier age in $Pold1^{+/L604K}$ mice, we used a Cox regression model to analyze the time to death in animals that died with histologically diagnosed tumors (3). We found that the hazard ratio (HR)—that is, the relative risk of dying with a tumor at any point in time—did not differ statistically significantly between wild-type and $Pold1^{+/L604G}$ mice for all tumors combined or for the subgroups of tumors analyzed. However, quite distinct results were obtained for the $Pold1^{+/L604K}$ mice, as illustrated in the curves in Fig. 6 showing the probability of death with different types of tumors as a function of time. As indicated, we found significantly elevated HRs for all tumors (HR, 2.44; 95% confidence interval [CI], 1.50 to 3.97; $P = 0.0003$); for lymphoreticular tumors (HR, 2.59; 95% CI, 1.29 to 5.15; $P = 0.007$); and for a combination of other tumors (bronchoalveolar tumors, sarcomas, other epithelial and mesenchymal tumors; HR, 2.75; 95% CI, 1.24 to 6.07; $P = 0.01$). Although hepatocellular tumors were frequent, the HR was not greater than that for wild-type controls. The analysis shows that $Pold1^{+/L604K}$ mice bearing histologically confirmed tumors died at a significantly younger age than wild-type mice, indicating that the $Pold1^{+/L604K}$ allele accelerated tumor formation and/or progression.

Nonneoplastic pathology in $Pold1^{+/L604G}$ and $Pold1^{+/L604K}$ mice. In addition to analyzing tumors from wild-type and mutant mice used for the life span study, we also performed an extensive assessment of nonneoplastic pathology. The most frequent lesions observed among the three genotypes, affecting major organ systems, are summarized in Table 3. As indicated, we noted no significant differences in disease incidence between the wild-type and mutant animals, with the exception of cardiomyopathy in the $Pold1^{+/L604G}$ mice ($P = 0.0011$, Fisher's exact test). We also observed no significant differences in the mean severity of lesions among genotypes (data not shown). The overall disease burden, including both neoplastic (Table 2) and nonneoplastic lesions (Table 3), did not differ, supporting the conclusion that the heterozygous L604G and L604K mutations cause only subtle phenotypes at the organismal level.

Heterozygosity at *Pold1* is maintained in tumors from mutant mice. We used three approaches to determine whether tumors from $Pold1^{+/L604G}$ or $Pold1^{+/L604K}$ mice undergo loss of heterozygosity at the *Pold1* locus. In the first two methods, we analyzed nine diverse high-grade tumors in which 90% to 95% of the cells were malignant based on histology. In the first approach, we reverse transcribed total mRNA, amplified Pol δ cDNA, and sequence the reverse transcription (RT)-PCR products to determine the percentage of mutant alleles based on peak height. We observed that the cDNA transcripts encoded approximately equal amounts of the mutant and wild-type alleles (data not

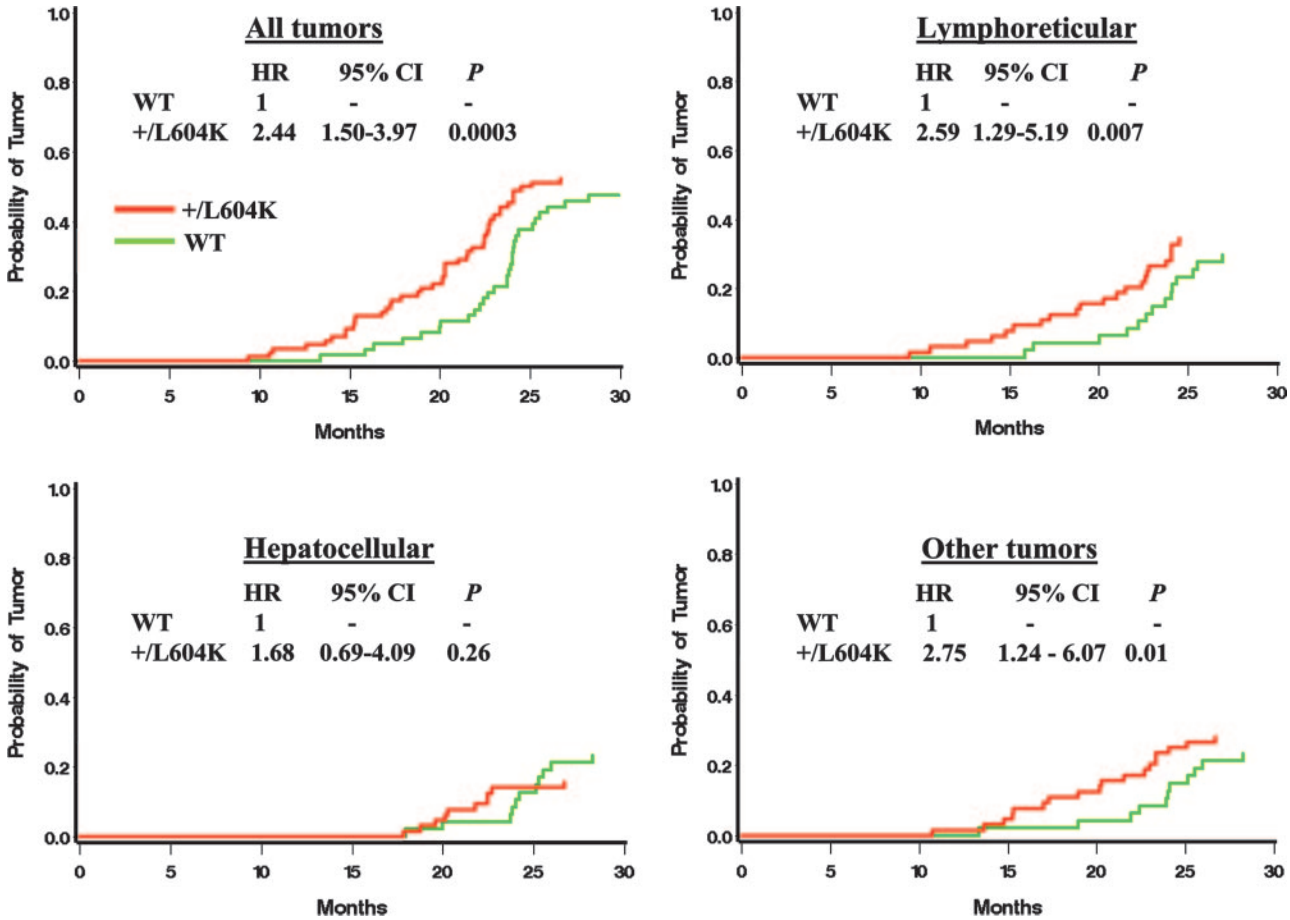

FIG. 6. Time to death with histologically diagnosed tumors. The risk of dying with a tumor as a function of time was analyzed by Cox regression analysis. In the *Pold1*$^{+/L604K}$ mice, the HRs were elevated for all tumors combined, for lymphoreticular tumors alone, and for all tumors excluding lymphoreticular and hepatocellular tumors (other tumors) but not for hepatocellular tumors. The latter tumors may be associated with *Helicobacter* infection. HRs for the four groups of tumors were not statistically significantly elevated in *Pold1*$^{+/L604G}$ mice, and probability curves are not shown. WT, wild type.

shown). In the second approach, the RT-PCR product was cloned into TA cloning vectors; 12 clones from each tumor sample were chosen at random, and nucleotides 1750 to 2250, which include the L604 codon, were sequenced. For each of the nine tumors, we found approximately equal numbers of clones containing the mutant and wild-type alleles (data not shown). In the third approach, we used a total of 12 tumors, including the 9 analyzed as described above. We genotyped strain-specific coding single-nucleotide polymorphisms (SNPs) at *Pold1* in the vicinity of the polymerase active site. These included two synonymous SNPs at positions encoding Asn528 and Thr536 and one nonsynonymous SNP encoding Gly or Ser at position 575. Since the genotype of the mice consists of a 50:50 mixture of

TABLE 3. Nonneoplastic pathology in *Pold1*$^{+/+}$, *Pold1*$^{+/L604G}$, and *Pold1*$^{+/L604K}$ mice[a]

Strain	No. of cases (incidence [%]) of:								
	Chronic hepatitis	Cardiomyopathy	Heart arteriosclerosis	Heart karyomegaly	Glomerulonephropathy	Acidophilic macrophage pneumonia	Spleen arteriosclerosis	Artery inflammation	Total nonneoplastic and neoplastic disease burden
Wild type	44 (76)	31 (56)	31 (36)	31 (65)	33 (54)	33 (17)	36 (11)	31 (9)	47 (87)
+/L604G	56 (77)	42 (88)	42 (31)	42 (76)	50 (62)	47 (34)	39 (13)	42 (10)	59 (88)
+/L604K	54 (72)	12 (83)	12 (33)	12 (75)	34 (75)	25 (36)	45 (20)	15 (27)	64 (94)

[a] Shown are the percentages of mice with the indicated pathology, diagnosed at the end of life. These nonneoplastic lesions were the most frequently noted in the study and were graded on a 0-to-4 severity scale, where 0 is normal or no change, 1 is minimal, 2 is mild, 3 is moderate, and 4 is marked or severe. To assign a numerical representation of the amount of disease present at the end of life, we summed the neoplastic burden (Table 2) and nonneoplastic lesions determined to be contributing to morbidity or mortality (grade 3 or higher) to generate the total disease burden.

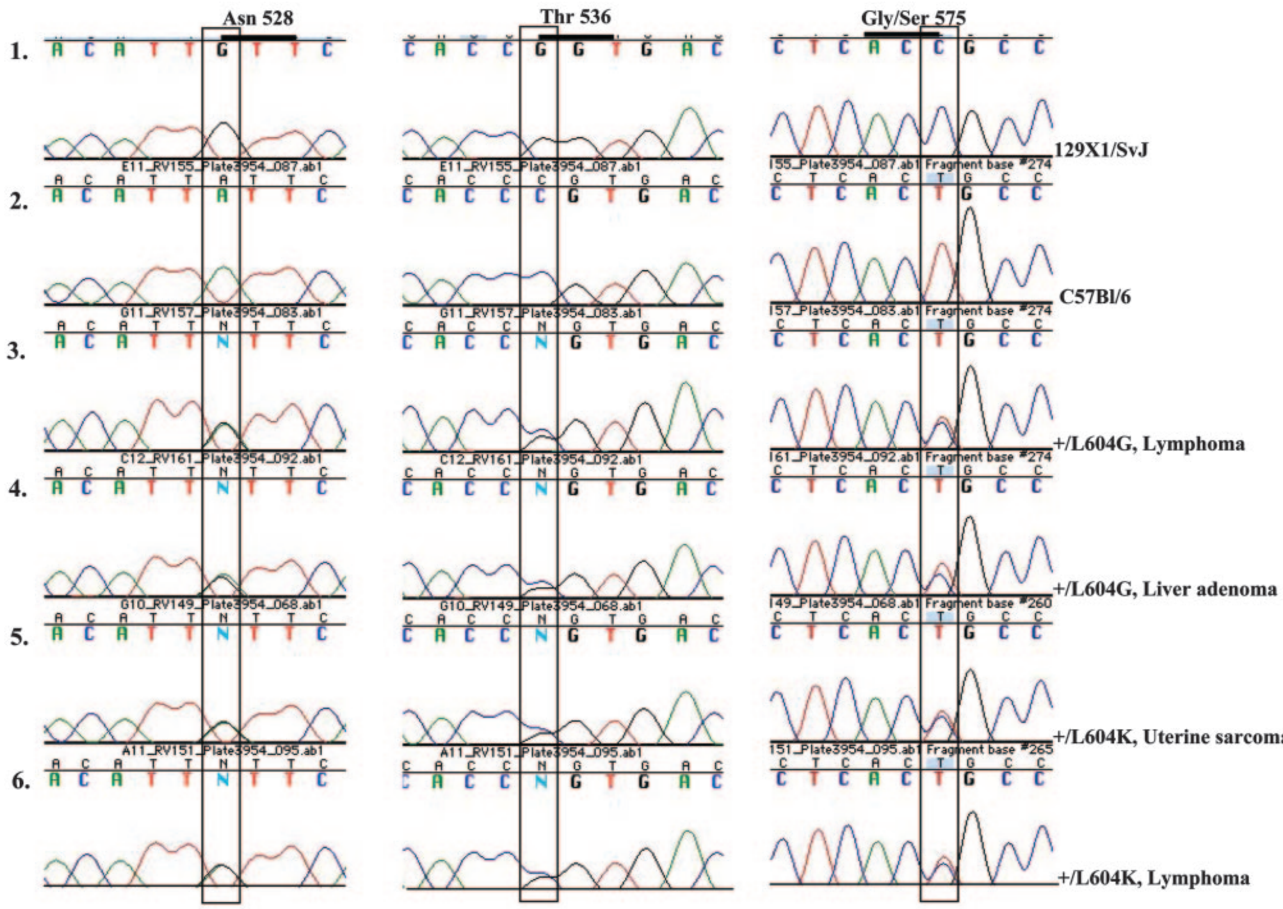

FIG. 7. No loss of heterozygosity at the *Pold1* locus in tumors from *Pold1*$^{+/L604G}$ and *Pold1*$^{+/L604K}$ mice. Mouse strain 129X1/SvJ- and C57BL/6-specific SNPs were genotyped at the *Pold1* locus in 12 histologically graded tumors from *Pold1*$^{+/L604K}$ and *Pold1*$^{+/L604G}$ mice; representative results for six tumors are shown. Tumors contained ~90% to 95% malignant cells. Genomic DNA was extracted and amplified with primers flanking exon 13 and intron 16 and sequenced. Sequence chromatograms are shown, and coding is by the complementary strand. Genotyped SNPs were as follows: 1, rs3720949 encoding Asn528, G in strain 129 and A in strain Bl6; 2, rs3720481 encoding Thr536, G in strain 129 and C in strain Bl6; 3, rs3719256 encoding position Gly/Ser575, C in strain 129 and T in strain Bl6. The 12 tumors analyzed included a follicular lymphoma, histiocytic sarcoma, hepatocellular adenoma, and hepatocellular carcinoma from *Pold1*$^{+/L604G}$ mice and a follicular lymphoma, mesenteric lymphoma, fibrosarcoma, uterine sarcoma, and hepatocellular carcinoma from *Pold1*$^{+/L604K}$ mice; these were also used for analysis of RT-PCR products (see Results). A histiocytic sarcoma and lymphocytic sarcoma from *Pold1*$^{+/L604G}$ mice and a lymphocytic sarcoma from a *Pold1*$^{+/L604K}$ mouse were analyzed in addition.

the Bl6 and 129 strains, differences in the peak heights of strain-specific nucleotides would indicate a change in copy number. As illustrated in Fig. 7, at the positions encoding Asn528 and Thr536, strain 129, which harbors the mutant *Pold1* alleles, has G at the wobble base panels (1, 3–6) whereas the wild-type allele in the Bl6 strain has adenine (A) and cytosine (C), respectively (panels 2 to 6). At the position encoding Gly/Ser575, strain 129 has C (panels 1 and 3 to 6) and the Bl6 strain has thymine (panels 2 to 6). We observed nearly equal peak heights of both the strain 129- and Bl6-specific nucleotides at all three positions among all of the 12 tumor samples, indicating that both the wild-type and mutant alleles are present. These results indicate that (i) loss of heterozygosity at the *Pold1* locus does not give rise to the tumors, (ii) neither the L604G nor the L604K allele is lost during tumor progression, and (iii) expression of the wild-type and mutant alleles is equivalent at the mRNA level. The results also imply that homozygosity for the mutant alleles, and/or hemizygosity for the wild-type allele, may be incompatible with cell viability.

DISCUSSION

The consequences for mammalian physiology of mutations in the polymerase domain of the essential replicative DNA polymerases α, δ, and ε have not yet been reported. In the present work, we examined the consequences of two mutations at a highly conserved residue in the polymerase active site of mouse Pol δ, L604G and L604K, that are homologous to mutations we previously analyzed in *S. cerevisiae* (62). Importantly, the phenotypes of haploid yeast cells suggest that both the mutant Pol δ alleles encode significantly compromised polymerases. Both alleles elevated forward mutation rates about 15-fold, encompassing increased base substitutions that are suggestive of compromised base discrimination. Both alleles increased hypersensitivity to hydroxyurea and methylmethane sulfonate, suggestive of a reduced capacity to tolerate replication stress, and both exhibited anomalous cell cycle progression, suggesting that replication is compromised even in the absence of exogenous agents. The latter two characteristics indicate that the mutant polymerases may have reduced catalytic activity and/or processivity. The serious defects in yeast physiology, together with the crucial role of Pol δ in genome replication, raised the question of whether mice harboring the homologous L604G and L604K mutations would be viable, and if so, the extent to which the mutations would be reflected in cellular and organismal phenotypes.

Viability, disease incidence, and life span. When homozygous, both the L604G and L604K alleles caused embryonic lethality. Failure of the homozygous mutant polymerases to sustain embryogenesis may be due to the requirement for rapid proliferation and calls to mind the anomalous cell cycle progression and reduced capacity of the homologous mutant yeast polymerases to tolerate replicative stress. Both the L604G and L604K heterozygous mutant mice are viable, appear to develop normally, are fertile, and do not exhibit a significant overall incidence of disease at the end of life (Table 3). The relative normalcy of the heterozygotes is indicative of remarkably effective compensation for the flawed synthesis catalyzed by the mutant polymerases, presumably effected by wild-type Pol δ and other DNA polymerases, by DNA repair and tolerance mechanisms, and perhaps by tissue-specific induction of apoptosis and additional processes. The longevity of L604 heterozygous mice is allele dependent, the median life span of *Pold1*$^{+/L604G}$ mice being the same as that of wild-type mice and that of *Pold1*$^{+/L60K}$ mice being modestly reduced (18%), a reduction that is likely due, at least in part, to accelerated tumorigenesis (Fig. 6). Given that the *Pold1*$^{+/L604G}$ and *Pold1*$^{+/L60K}$ MEFs show comparable increases in both the spontaneous mutation rate (Table 1) and chromosome aberrations (Fig. 3), the difference in life span suggests that the types and/or relative proportion of replication defects catalyzed by the L604K polymerase may be more deleterious or less well compensated by the wild-type polymerase and other mechanisms.

Mutator phenotypes of heterozygous *Pold1*$^{+/L604G}$ and *Pold1*$^{+/L604K}$ cells. The L604G and L604K alleles conferred mutator phenotypes at both the nucleotide and chromosome levels in heterozygous MEFs. The ca. fivefold increases in the spontaneous mutation rate at the *Hprt* locus (Table 1) may reflect both defective synthesis by the mutant enzymes, encompassing reduced base discrimination, catalytic efficiency, and/or processivity, as well as secondary mutagenic processes resulting from flawed replication. It is likely that the polymerase active site in the mutant enzymes generates more errors than the measured mutation rates indicate, due to proofreading at the exonuclease active site of Pol δ and other DNA polymerases, and to error correction by mismatch repair and perhaps additional exonucleases (1, 27, 56). We also observed 17- and 38-fold increases in chromosome anomalies in heterozygous L604G and L604K cells, respectively, due primarily to chromatid/chromosome breaks and gaps (Fig. 3). These aberrations are believed to result from stalling and collapse of replication forks, and in fact, much of the mutagenesis we observed may result from the processing of stalled or collapsed forks (21, 54). Unrepaired chromatid/chromosome gaps and breaks can lead to fusion, translocation, inversion, and amplification that contributes to tumorigenesis (23).

Replication fork collapse and attendant double-strand breaks can induce activation of S-phase checkpoint pathways (39). The histone H2AX is rapidly phosphorylated (γ-H2AX) after checkpoint activation, forming foci at chromatin sites proximal to the double-strand breaks and thus marking the sites of damage for recruitment/maintenance of DNA repair proteins (4, 15, 30, 59, 63). The mutator phenotype of heterozygous *Pold1*$^{+/L604G}$ and *Pold1*$^{+/L604K}$ mice suggests that the cells may sustain elevated replication stress, either spontaneously or in response to replication inhibition. By using FACS analysis, we observed that MEFs from *Pold1*$^{+/L604G}$ and *Pold1*$^{+/L604K}$ mice exhibit levels of γ-H2AX that do not differ from that of wild-type MEFs, both with and without exposure to the replication inhibitors aphidicolin and hydroxyurea (Fig. 4). We infer that wild-type Pol δ in the heterozygous L604G and L604K cells, together with additional mechanisms that include Pol ε, efficiently compensates for defects associated with the mutant DNA polymerase, thus maintaining a wild-type steady-state level of γ-H2AX phosphorylation.

Tumorigenesis in heterozygous mice. Neither the *Pold1*$^{+/L604G}$ nor the *Pold1*$^{+/L604K}$ cohort displayed a significant increase in tumor incidence (Table 2), although the incidence in *Pold1*$^{+/L604K}$ mice may be underestimated, as described in Results. The tumors observed in heterozygous mutant animals included those of mesenchymal origin, such as lymphoreticular tumors (lymphomas) and those of epithelial origin, such as lung adenomas and carcinomas (Table 2), all commonly seen in Bl6 × 129 mice (20). We also observed an unusually high incidence of hepatocellular adenomas and carcinomas in the wild-type and mutant animals, relative to that reported for the Bl6 × 129 strain (20; data not shown). The development of hepatocellular adenomas and carcinomas in our mice may be related to *Helicobacter* infection (31, 32, 51). We detected the presence of *Helicobacter hepaticus* and *Helicobacter bilis* in fecal matter by PCR assay.

Regression analysis showed that the age-dependent probability of dying with a histologically diagnosed tumor was significantly increased in the heterozygous L604K versus wild-type mice (Fig. 6). The data thus indicate that the L604K allele accelerated death from cancer, presumably via replication defects that promote tumor formation and/or progression. Even though the mutator phenotypes we observed for both *Pold1*$^{+/L604G}$ and *Pold1*$^{+/L604K}$ MEFs are similar in magnitude, the *Pold1*$^{+/L604G}$ mice did not exhibit a detectable cancer phenotype. As in the case of life span, the allele dependence presumably reflects differences in the types and relative proportions of replication defects catalyzed by the mutant polymerases and/or differential compensation. Preliminary experiments (K. Albertson and B. Preston) indicate that *Pold1*$^{+/L604G}$ *Msh2*$^{-/-}$ mice lacking mismatch repair exhibit increased tumorigenesis relative to *Pold1*$^{+/L604G}$, *Msh2*$^{-/-}$, or wild-type mice. The data suggest that mismatch repair can suppress the tumorigenic potential of the *Pold1*$^{+/L604G}$ allele and that unrepaired base substitution errors made by the L604G polymerase can produce a cancer phenotype.

Loss of heterozygosity is frequent in murine and human cancers (64). Loss of heterozygosity occurs at many loci in sporadic tumors and in tumors associated with inherited diseases characterized by increased cancer incidence. Germ line heterozygosity at certain loci, e.g., *Rb*, can accelerate loss of the wild-type allele and promote tumorigenesis (26). In the case of tumors from heterozygous *Pold1*$^{+/L604G}$ or *Pold1*$^{+/L604K}$ mice, we observed retention of both the wild-type and mutant alleles in 12 high-grade tumors, indicating that loss of heterozygosity does not contribute to tumorigenesis and suggesting that neither reduction to homozygosity for the mutant allele nor hemizygosity for the wild-type allele is compatible with tumor growth.

Mutation in the Pol δ polymerase and exonuclease domains generates different phenotypes. The phenotypes thus far associated with mutation in the murine Pol δ exonuclease and polymerase active sites differ considerably. Unlike mice carrying a homozygous L604G or L604K mutations that die in utero, mice carrying a mutation (D400A) in the Pol δ exonuclease domain that essentially abolishes proofreading are viable, appear to develop normally, and are fertile (16, 17). This major difference between the homozygous exonuclease-deficient and heterozygous L604 mutant mice presumably arises from the nature and extent of the mutations caused in the respective animals and may reflect compromised activity and/or processivity of the mutant L604 polymerases and concomitant replication defects. Inactivating mutations at the exonuclease active site have been shown to have minimal effects on polymerase activity; in the case of yeast Pol δ, for example, no measurable reduction was detected (25). Unlike the L604K and L604G heterozygous MEFs, *Pold1*$^{D400A/D400A}$ MEFs do not display significant chromosome instability (B. Preston, unpublished data), suggesting that the chromosome aberrations seen in the mutant L604 MEFs do not derive from base substitution errors. *Pold1*$^{D400A/D400A}$ MEFs do have a mutator phenotype, exhibiting an ca. 15-fold increase in the rate of spontaneous mutation to ouabain resistance that presumptively derives from unrepaired base substitution errors (16). *Pold1*$^{D400A/D400A}$ mice have reduced longevity, with a median survival of ca. 10 months (16). They also have a strong cancer phenotype that differs from that of the heterozygous L604K mice, dying of lymphomas at an early age and also displaying a high incidence of epithelial cancers that includes unusual squamous cell carcinomas of the skin (16). The origins of the different tumor spectra are unclear. Heterozygous *Pold1*$^{+/D400A}$ mice have a weaker mutator phenotype than do the homozygous *Pold1*$^{D400A/D400A}$ mice. They are like wild-type mice with respect to longevity and tumor incidence, suggestive of efficient compensation for the errors made by the exonuclease-deficient polymerase.

Structure-function relationships in the mutant DNA polymerases. We lack information concerning a structural basis for the apparent reduction in the accuracy and catalytic efficiency of the mutant L604G and L604K polymerases. The crystal structure of a closed ternary complex of the homologous phage RB69 gp43 DNA polymerase with DNA and an incoming dNTP (Fig. 1A and 3B) (12) shows that the side chain of wild-type Leu at position 415 is in close proximity to the sugar and α-phosphate of the incoming nucleotide. Modeling of the L415G and L415K substitutions in the RB69 DNA polymerase complex (Fig. 1C II) shows that both mutant residues are accommodated without obvious changes in active-site geometry or side chain interactions that might account for reduced base discrimination or other defects in catalysis. The absence of a side chain in the L415G polymerase allows greater space and perhaps flexibility for accommodation of incorrect base pairs, but this alone is unlikely to explain our observations in mutant mice. We have speculated that replacements at L612 in yeast Pol δ may affect partitioning between the polymerase and exonuclease sites, and recent biochemical analysis in the Kunkel laboratory indicates that this is the case for the L612M polymerase (33).

Implications for human carcinogenesis. Our data show that a single mutation in the polymerase active site of mammalian Pol δ can cause mutator and cancer phenotypes. These findings are in accord with the mutator phenotype hypothesis, which states that normal mutation rates are too low to account for the large numbers of mutations seen in human cancers and hence that cancers must sustain increased mutation rates at some time in their evolution (29). This hypothesis, as first formulated, suggested that inaccurate DNA polymerases or deficits in DNA repair might be responsible for increased mutation. We now know that a multitude of genes that control the integrity of DNA are mutated in human tumors, although a causal relationship has been established only for some. The mutated genes that have been found in human cancers affect DNA repair, the DNA damage response, chromosome segregation, and apoptosis, among other processes (13). Yet, interestingly, the ongoing search for mutations in human tumors has yielded few alterations in the genes for replicative DNA polymerases (13). In the case of Pol δ, sequencing of cDNA has revealed seven point mutations and two single-nucleotide deletions among six colon cancer cell lines and three identical point mutations among seven sporadic colon cancers (6, 10, 45). A single point mutation in Pol α in a malignant melanoma has also been reported in the COSMIC database, http://www.sanger.ac.uk/genetics/CGP/cosmic/. This relative paucity of mutations may reflect the reasonable presumption that many mutant replicative polymerases may be too compromised to sustain rapid proliferation, perhaps due to defective polymerization or diminished stability, and are therefore selected against during clonal evolution of tumors.

In summary, it is unknown how prevalent mutant replicative polymerases are in human cancers and whether they are a source of the mutations required for carcinogenesis or of tumor heterogeneity at the DNA and cellular levels. However, our present findings demonstrate that mutations in the polymerase domain of DNA Pol δ are compatible with a high level of cellular function and can give rise to tumors and/or accelerate tumorigenesis.

ACKNOWLEDGMENTS

This work was supported by National Institutes of Health grants RO1 CA102029, RO1 CA78885, and PO11 AG01751 to L.A.L.; RO1 CA98242 and PO11 AG01751 to B.D.P.; and U01 ES11045 to W.C.L.

We are grateful to Ann Blank for editing the manuscript and for technical comments and to Elinor Adman for advice and the generation of molecular modeling figures. We thank the entire University of Washington Transgenic Mouse Core under the leadership of W.C.L., particularly Carol Ware, John Morton, Ruby Sue Mangalindan, and La'Akea Siverts. We also thank Peter Rabinovitch and Mike Shen for expert guidance in FACS analysis.

REFERENCES

1. **Albertson, T. M., and B. D. Preston.** 2006. DNA replication fidelity: proofreading in trans. Curr. Biol. **16:**R209–R211.
2. **Bebenek, K., C. M. Joyce, M. P. Fitzgerald, and T. A. Kunkel.** 1990. The fidelity of DNA synthesis catalyzed by derivatives of Escherichia coli DNA polymerase I. J. Biol. Chem. **265:**13878–13887.
3. **Bland, M.** 1995. An introduction to medical statistics, 2nd ed. Oxford University Press, Oxford, United Kingdom.
4. **Burma, S., B. P. Chen, M. Murphy, A. Kurimasa, and D. J. Chen.** 2001. ATM phosphorylates histone H2AX in response to DNA double-strand breaks. J. Biol. Chem. **276:**42462–42467.
5. **Cullmann, G., R. Hindges, M. W. Berchtold, and U. Hubscher.** 1993. Cloning of a mouse cDNA encoding DNA polymerase delta: refinement of the homology boxes. Gene **134:**191–200.
6. **da Costa, L. T., B. Liu, W. el-Deiry, S. R. Hamilton, K. W. Kinzler, B. Vogelstein, S. Markowitz, J. K. Willson, A. de la Chapelle, K. M. Downey, et al.** 1995. Polymerase delta variants in RER colorectal tumours. Nat. Genet. **9:**10–11.
7. **Datta, A., J. L. Schmeits, N. S. Amin, P. J. Lau, K. Myung, and R. D. Kolodner.** 2000. Checkpoint-dependent activation of mutagenic repair in Saccharomyces cerevisiae pol3-01 mutants. Mol. Cell **6:**593–603.
8. **Dong, Q., W. C. Copeland, and T. S. Wang.** 1993. Mutational studies of human DNA polymerase alpha. Identification of residues critical for deoxynucleotide binding and misinsertion fidelity of DNA synthesis. J. Biol. Chem. **268:**24163–24174.
9. **Engh, R. A. and R. Huber.** 1991. Accurate bond and angle parameters for X-ray protein structure refinement. Acta Crystallogr. Sect. A Found. Crystallogr. **47:**392–400.
10. **Flohr, T., J. C. Dai, J. Buttner, O. Popanda, E. Hagmuller, and H. W. Thielmann.** 1999. Detection of mutations in the DNA polymerase delta gene of human sporadic colorectal cancers and colon cancer cell lines. Int. J. Cancer **80:**919–929.
11. **Fortune, J. M., Y. I. Pavlov, C. M. Welch, E. Johansson, P. M. Burgers, and T. A. Kunkel.** 2005. Saccharomyces cerevisiae DNA polymerase delta: high fidelity for base substitutions but lower fidelity for single- and multi-base deletions. J. Biol. Chem. **280:**29980–29987.
12. **Franklin, M. C., J. Wang, and T. A. Steitz.** 2001. Structure of the replicating complex of a pol alpha family DNA polymerase. Cell **105:**657–667.
13. **Futreal, P. A., L. Coin, M. Marshall, T. Down, T. Hubbard, R. Wooster, N. Rahman, and M. R. Stratton.** 2004. A census of human cancer genes. Nat. Rev. Cancer **4:**177–183.
14. **Garg, P., and P. M. Burgers.** 2005. DNA polymerases that propagate the eukaryotic DNA replication fork. Crit. Rev. Biochem. Mol. Biol. **40:**115–128.
15. **Goldberg, M., M. Stucki, J. Falck, D. D'Amours, D. Rahman, D. Pappin, J. Bartek, and S. P. Jackson.** 2003. MDC1 is required for the intra-S-phase DNA damage checkpoint. Nature **421:**952–956.
16. **Goldsby, R. E., L. E. Hays, X. Chen, E. A. Olmsted, W. B. Slayton, G. J. Spangrude, and B. D. Preston.** 2002. High incidence of epithelial cancers in mice deficient for DNA polymerase delta proofreading. Proc. Natl. Acad. Sci. USA **99:**15560–15565.
17. **Goldsby, R. E., N. A. Lawrence, L. E. Hays, E. A. Olmsted, X. Chen, M. Singh, and B. D. Preston.** 2001. Defective DNA polymerase-delta proofreading causes cancer susceptibility in mice. Nat. Med. **7:**638–639.
18. **Goldsby, R. E., M. Singh, and B. D. Preston.** 1998. Mouse DNA polymerase delta gene (Pold1) maps to chromosome 7. Mamm. Genome **9:**92–93.
19. **Greene, C. N., and S. Jinks-Robertson.** 2001. Spontaneous frameshift mutations in Saccharomyces cerevisiae: accumulation during DNA replication and removal by proofreading and mismatch repair activities. Genetics **159:**65–75.
20. **Haines, D. C., S. Chattopadhyay, and J. M. Ward.** 2001. Pathology of aging B6;129 mice. Toxicol. Pathol. **29:**653–661.
21. **Helleday, T.** 2003. Pathways for mitotic homologous recombination in mammalian cells. Mutat. Res. **532:**103–115.
22. **Hubscher, U., G. Maga, and S. Spadari.** 2002. Eukaryotic DNA polymerases. Annu. Rev. Biochem. **71:**133–163.
23. **Huret, J. L., S. Senon, A. Bernheim, and P. Dessen.** 2004. An atlas on genes and chromosomes in oncology and haematology. Cell. Mol. Biol. (Noisy-le-Grand). **50:**805–807.
24. **Ikeno, Y., R. T. Bronson, G. B. Hubbard, S. Lee, and A. Bartke.** 2003. Delayed occurrence of fatal neoplastic diseases in Ames dwarf mice: correlation to extended longevity. J. Gerontol. A Biol. Sci. Med. Sci. **58:**291–296.
25. **Jin, Y. H., R. Ayyagari, M. A. Resnick, D. A. Gordenin, and P. M. Burgers.** 2003. Okazaki fragment maturation in yeast. II. Cooperation between the polymerase and 3′-5′-exonuclease activities of Pol delta in the creation of a ligatable nick. J. Biol. Chem. **278:**1626–1633.
26. **Knudson, A. G., Jr.** 1971. Mutation and cancer: statistical study of retinoblastoma. Proc. Natl. Acad. Sci. USA **68:**820–823.
27. **Kunkel, T. A., and D. A. Erie.** 2005. DNA mismatch repair. Annu. Rev. Biochem. **74:**681–710.
28. **Li, L., K. M. Murphy, U. Kanevets, and L. J. Reha-Krantz.** 2005. Sensitivity to phosphonoacetic acid: a new phenotype to probe DNA polymerase delta in Saccharomyces cerevisiae. Genetics **170:**569–580.
29. **Loeb, L. A., K. R. Loeb, and J. P. Anderson.** 2003. Multiple mutations and cancer. Proc. Natl. Acad. Sci. USA **100:**776–781.
30. **Lou, Z., K. Minter-Dykhouse, X. Wu, and J. Chen.** 2003. MDC1 is coupled to activated CHK2 in mammalian DNA damage response pathways. Nature **421:**957–961.
31. **Maggio-Price, L., H. Bielefeldt-Ohmann, P. Treuting, B. M. Iritani, W. Zeng, A. Nicks, M. Tsang, D. Shows, P. Morrissey, and J. L. Viney.** 2005. Dual infection with Helicobacter bilis and Helicobacter hepaticus in p-glycoprotein-deficient mdr1a$^{-/-}$ mice results in colitis that progresses to dysplasia. Am. J. Pathol. **166:**1793–1806.
32. **Maggio-Price, L., P. Treuting, W. Zeng, M. Tsang, H. Bielefeldt-Ohmann, and B. M. Iritani.** 2006. Helicobacter infection is required for inflammation and colon cancer in SMAD3-deficient mice. Cancer Res. **66:**828–838.
33. **McElhinny, S. A., C. M. Stith, P. M. Burgers, and T. A. Kunkel.** 2007. Inefficient proofreading and biased error rates during inaccurate DNA synthesis by a mutant derivative of Saccharomyces cerevisiae DNA polymerase delta. J. Biol. Chem. **282:**2324–2332.
34. **Minnick, D. T., K. Bebenek, W. P. Osheroff, R. M. Turner, Jr., M. Astatke, L. Liu, T. A. Kunkel, and C. M. Joyce.** 1999. Side chains that influence fidelity at the polymerase active site of Escherichia coli DNA polymerase I (Klenow fragment). J. Biol. Chem. **274:**3067–3075.
35. **Morrison, A., A. L. Johnson, L. H. Johnston, and A. Sugino.** 1993. Pathway correcting DNA replication errors in Saccharomyces cerevisiae. EMBO J. **12:**1467–1473.
36. **Morrison, A., and A. Sugino.** 1994. The 3′→5′ exonucleases of both DNA polymerases delta and epsilon participate in correcting errors of DNA replication in Saccharomyces cerevisiae. Mol. Gen. Genet. **242:**289–296.
37. **Nagy, A., J. Rossant, R. Nagy, W. Abramow-Newerly, and J. C. Roder.** 1993. Derivation of completely cell culture-derived mice from early-passage embryonic stem cells. Proc. Natl. Acad. Sci. USA **90:**8424–8428.
38. **Niimi, A., S. Limsirichaikul, S. Yoshida, S. Iwai, C. Masutani, F. Hanaoka, E. T. Kool, Y. Nishiyama, and M. Suzuki.** 2004. Palm mutants in DNA polymerases alpha and eta alter DNA replication fidelity and translesion activity. Mol. Cell. Biol. **24:**2734–2746.
39. **Osborn, A. J., S. J. Elledge, and L. Zou.** 2002. Checking on the fork: the DNA-replication stress-response pathway. Trends Cell Biol. **12:**509–516.
40. **Patel, P. H., H. Kawate, E. Adman, M. Ashbach, and L. A. Loeb.** 2001. A single highly mutable catalytic site amino acid is critical for DNA polymerase fidelity. J. Biol. Chem. **276:**5044–5051.
41. **Patel, P. H., and L. A. Loeb.** 2000. Multiple amino acid substitutions allow DNA polymerases to synthesize RNA. J. Biol. Chem. **275:**40266–40272.
42. **Pavlov, Y. I., P. V. Shcherbakova, and T. A. Kunkel.** 2001. In vivo consequences of putative active site mutations in yeast DNA polymerases alpha, epsilon, delta, and zeta. Genetics **159:**47–64.
43. **Pavlov, Y. I., P. V. Shcherbakova, and I. B. Rogozin.** 2006. Roles of DNA polymerases in replication, repair, and recombination in eukaryotes. Int. Rev. Cytol. **255:**41–132.
44. **Polesky, A. H., T. A. Steitz, N. D. Grindley, and C. M. Joyce.** 1990. Identification of residues critical for the polymerase activity of the Klenow fragment of DNA polymerase I from Escherichia coli. J. Biol. Chem. **265:**14579–14591.
45. **Popanda, O., T. Flohr, G. Fox, and H. W. Thielmann.** 1999. A mutation detected in DNA polymerase delta cDNA from Novikoff hepatoma cells correlates with abnormal catalytic properties of the enzyme. J. Cancer Res. Clin. Oncol. **125:**598–608.
46. **Prelich, G., C. K. Tan, M. Kostura, M. B. Mathews, A. G. So, K. M. Downey, and B. Stillman.** 1987. Functional identity of proliferating cell nuclear antigen and a DNA polymerase-delta auxiliary protein. Nature **326:**517–520.
47. **Reha-Krantz, L. J., and R. L. Nonay.** 1994. Motif A of bacteriophage T4 DNA polymerase: role in primer extension and DNA replication fidelity. Isolation of new antimutator and mutator DNA polymerases. J. Biol. Chem. **269:**5635–5643.
48. **Rogakou, E. P., C. Boon, C. Redon, and W. M. Bonner.** 1999. Megabase chromatin domains involved in DNA double-strand breaks in vivo. J. Cell Biol. **146:**905–916.
49. **Rogakou, E. P., W. Nieves-Neira, C. Boon, Y. Pommier, and W. M. Bonner.** 2000. Initiation of DNA fragmentation during apoptosis induces phosphorylation of H2AX histone at serine 139. J. Biol. Chem. **275:**9390–9395.
50. **Rogakou, E. P., D. R. Pilch, A. H. Orr, V. S. Ivanova, and W. M. Bonner.** 1998. DNA double-stranded breaks induce histone H2AX phosphorylation on serine 139. J. Biol. Chem. **273:**5858–5868.
51. **Rogers, A. B., S. R. Boutin, M. T. Whary, N. Sundina, Z. Ge, K. Cormier, and J. G. Fox.** 2004. Progression of chronic hepatitis and preneoplasia in Helicobacter hepaticus-infected A/JCr mice. Toxicol. Pathol. **32:**668–677.
52. **Rosenkranz, H. S., and J. A. Levy.** 1965. Hydroxyurea: a specific inhibitor of deoxyribonucleic acid synthesis. Biochim. Biophys. Acta **95:**181–183.
53. **Rossman, T. G., E. I. Goncharova, and A. Nadas.** 1995. Modeling and measurement of the spontaneous mutation rate in mammalian cells. Mutat. Res. **328:**21–30.
54. **Saleh-Gohari, N., H. E. Bryant, N. Schultz, K. M. Parker, T. N. Cassel, and**

T. Helleday. 2005. Spontaneous homologous recombination is induced by collapsed replication forks that are caused by endogenous DNA single-strand breaks. Mol. Cell. Biol. **25:**7158–7169.
55. **Schaaper, R. M.** 1993. Base selection, proofreading, and mismatch repair during DNA replication in Escherichia coli. J. Biol. Chem. **268:**23762–23765.
56. **Shevelev, I. V., and U. Hubscher.** 2002. The 3′ 5′ exonucleases. Nat. Rev. Mol. Cell. Biol. **3:**364–376.
57. **Shinkai, A., P. H. Patel, and L. A. Loeb.** 2001. The conserved active site motif A of Escherichia coli DNA polymerase I is highly mutable. J. Biol. Chem. **276:**18836–18842.
58. **Simon, M., L. Giot, and G. Faye.** 1991. The 3′ to 5′ exonuclease activity located in the DNA polymerase delta subunit of Saccharomyces cerevisiae is required for accurate replication. EMBO J. **10:**2165–2170.
59. **Stewart, G. S., B. Wang, C. R. Bignell, A. M. Taylor, and S. J. Elledge.** 2003. MDC1 is a mediator of the mammalian DNA damage checkpoint. Nature **421:**961–966.
60. **Suzuki, M., A. K. Avicola, L. Hood, and L. A. Loeb.** 1997. Low fidelity mutants in the O-helix of Thermus aquaticus DNA polymerase I. J. Biol. Chem. **272:**11228–11235.
61. **Tan, C. K., C. Castillo, A. G. So, and K. M. Downey.** 1986. An auxiliary protein for DNA polymerase-delta from fetal calf thymus. J. Biol. Chem. **261:**12310–12316.
62. **Venkatesan, R. N., J. J. Hsu, N. A. Lawrence, B. D. Preston, and L. A. Loeb.** 2006. Mutator phenotypes caused by substitution at a conserved motif A residue in eukaryotic DNA polymerase delta. J. Biol. Chem. **281:**4486–4494.
63. **Ward, I. M., and J. Chen.** 2001. Histone H2AX is phosphorylated in an ATR-dependent manner in response to replicational stress. J. Biol. Chem. **276:**47759–47762.
64. **Weinberg, R. A.** 2007. The biology of cancer. Garland Science, New York, NY.
65. **Wright, G. E., U. Hubscher, N. N. Khan, F. Focher, and A. Verri.** 1994. Inhibitor analysis of calf thymus DNA polymerases alpha, delta and epsilon. FEBS Lett. **341:**128–130.